ELSEVIER

Marine Chemistry 62 (1998) 65–76

MARINE CHEMISTRY

Potential interactions between sedimentary dissolved organic matter and mineral surfaces

Crystal A. Thimsen, Richard G. Keil *

University of Washington, School of Oceanography, Box 357940, Seattle, WA 98195-7940 USA

Received 1 April 1997; revised 11 January 1998; accepted 20 January 1998

Abstract

The sorptive properties of pore water organic matter and organic matter easily extracted from marine sediments were examined in a series of batch adsorption and desorption experiments. Pore water natural organic matter (*p*NOM) and easily extracted natural organic matter (*e*NOM) were isolated from Sinclair Inlet, WA (USA) sediments. The NOM fractions were concentrated ~9 times via rotoevaporation and then sorbed to, and desorbed from, organic-free sediment, sediment size fractions (63–250, 38–63 and <38 μm), montmorillonite and iron oxide. Sorption isotherms of *p*NOM varied little with changing sediment grain size or mineralogy, and Freundlich linearity coefficients (*n*) were all near 1 (range 0.65–1.15). *e*NOM was more heterogeneous in its sorption to the various surfaces, having a wider range of linearity coefficients (0.38–1.36) and a greater tendency to sorb to the montmorillonite. Average partition coefficients (K_d) for the *p*NOM and *e*NOM were small (0.1 ± 0.04 and 0.08 ± 0.03 l g^{-1}), illustrating only a low affinity for the surfaces. Hystereses observed in the desorption isotherms relative to the adsorption isotherms extrapolate back to the origin, suggesting that the sorption of NOM was reversible. A multiple-component model fit to the sorption and desorption data suggests that both the *p*NOM and *e*NOM fractions can be described as ~1:2 mixtures of two components with average K_d's of 3.2 and 0.02 l g^{-1}, respectively. This result was confirmed in a cumulative adsorption experiment, where less than 40% of the *p*NOM was found to be surface-reactive. The overall similarity of the sorptive properties of *p*NOM and *e*NOM suggest that the two isolates are subgroups of a single sedimentary NOM pool. At natural sediment porosities between 0.5 and 0.95, *p*NOM is buffered by a surface-bound *e*NOM pool that is many times larger than the *p*NOM pool with which it is undergoing exchange.

Keywords: organic matter; mineral surfaces; sediment; adsorption

1. Introduction

Sorption to particle surfaces can play an important role in controlling the distribution and bioavailability of many organic compounds in aquatic systems (Sugai and Henrichs, 1992; Gordon and Millero, 1985; Gu et al., 1996). In marine sediments this may be of general importance because spatial surveys show a strong relationship between mineral surface area and total organic matter content (Mayer, 1994; Keil et al., 1994; Hedges and Keil, 1995) that is consistent with most organic matter in coastal marine sediments being sorbed to mineral surfaces. If this is the case, then a significant fraction of the sedimentary organic matter could have passed through the

* Corresponding author. Tel.: +1-206-616-1947. E-mail: rickkeil@ocean.washington.edu

0304-4203/98/$19.00
PII S0304-4203(98)00018-8

dissolved phase before undergoing remineralization, diffusion (out of the sediment) or sorption (Hedges and Keil, 1995; Pedersen, 1995).

Although the surface reactivity of many specific organic molecules in sea water is known (Hedges, 1977; Sansone et al., 1987; Kirchman et al., 1989; Henrichs and Sugai, 1993; Wang and Lee, 1993), the general surface reactivity of natural organic matter in pore waters (pNOM) is not. Hypothetically, pNOM should contain components that are not surface reactive as well as marginally surface reactive components that are buffered by their sorbed counterparts (and presumably undergoing constant thermodynamic exchange). While components with high partition coefficients may be present, their concentrations in pNOM would presumably be only a small percentage of the total pore water organic pool except under extreme conditions (Henrichs, 1995). For example, in a sediment with a porosity of 0.75 and three organic components in equal proportions with partition coefficients (l kg^{-1}) of $A = 0.01$, $B = 0.1$ and $C = 1.0$, at steady state the pNOM would be composed of 89% component A, 10% B and 1% C.

This study specifically aimed to investigate the surface reactivity of pNOM and the NOM that could be easily extracted from the mineral matrix using organic-free sea water (eNOM). It was hypothesized that the two NOM fractions would be similar in surface reactivity, and that eNOM might be a component in exchange with a fraction of the pNOM. We did not attempt to investigate the tightly associated organic matter. Our observations indicate that pNOM and eNOM associations with mineral surfaces are largely reversible and that the pNOM and eNOM phases have similar affinities for mineral surfaces and similar desorption profiles.

2. Materials and methods

Sediment was collected at the Sinclair Inlet Natural Wildlife Observatory, Puget Sound, WA, USA. Sinclair Inlet is a small semi-enclosed, partially mixed marine embayment on the eastern edge of the Olympic Peninsula with a maximum water depth of 50 m and seasonal salinity variations of 24 to 30‰. Freshwater input to Sinclair Inlet is limited to soil run-off and one small creek. Sediment in the inlet is predominately coarse to fine silt (60%) with moderate sand (25%) and clay (15%) contents (based on mass). Sediment and sediment pore water was collected in the tidal flat during a neap tide on August 14, 1995 at the south-western edge of the inlet. The sampling location was at the low water boundary, and thus the sediment interface was exposed to air only monthly rather than daily. Teflon spatulas were used to collect sediment which was placed in cleaned polypropylene containers and transported directly to the laboratory. Approximately 16 kg of sediment was collected. Sediment was stored at 10°C overnight until pore water extraction began. All glassware was cleaned with a sodium phosphate solution, rinsed with distilled water, and muffled at 400°C for 12 h. All plastic ware (polycarbonate centrifuge tubes, Teflon transfer vials, etc.) was cleaned with the phosphate solution, rinsed copiously with distilled water, soaked overnight in a 10% HCl bath and rinsed again.

2.1. Pore water extraction and NOM concentration

Pore water was separated from sediment via centrifugation at $3500 \times g$ for 15 min in 250 ml polycarbonate centrifuge tubes using a Sorvall SS-3 centrifuge. Following removal of the pore water, an equivalent volume of ultraviolet-oxidized sea water (25‰ salinity) was added to the tubes and the tubes were homogenized, allowed to sit for 1 h in a refrigerator and centrifuged again. Total pore water and extracted water volumes were approximately 4.5 l each. The pNOM and eNOM solutions were poisoned with $HgCl_2$ at a final concentration of 0.001 g l^{-1} (before rotoevaporation—see below) to prevent microbial growth (Wang and Lee, 1993) and stored separately at 2°C. Although $HgCl_2$ is a strong complexing agent and could potentially influence NOM sorption, concern about microbial effects on sorption prompted use of the poison. In a control experiment using NOM sterilized by ultrafiltration with and without added poison, no adverse effect on sorption was observed when using the $HgCL_2$ (Keil, unpublished data). Similar results were observed by Wang and Lee (1993). The lack of a measurable Hg–NOM complexation effect may be due to complexation of the added mercury with Cl and competition between added Hg and the Ca and Mg ions in seawater for NOM binding sites.

Table 1
Pore water and extracted water salinities, NOM concentrations and $C:N_{atomic}$ ratios, and concentration factors (Cf) for materials isolated from Sinclair Inlet sediments

	Initial DOC mg C l^{-1}	Final DOC mg C l^{-1}	Cf	$(C:N)_a$	Initial Salinity (‰)	Final Salinity (‰)	Cf	Initial sediment porosity
*p*NOM	15.3 ± 0.03	138 ± 3	9.0	17.5 ± 1.2	24	220	9.2	0.49
*e*NOM	20.6 ± 0.2	175 ± 9	8.6	17.8 ± 3.7	24	210	8.7	0.49

After isolation, the NOM extracts were concentrated by rotoevaporation. Prior to concentration, a Millipore Minitan tangential-flow ultrafiltration unit fitted with a 0.2 μm filter was used to eliminate large material. The *p*NOM and *e*NOM had initial dissolved organic carbon (DOC) concentrations of 15.3 ± 0.03 mg C l^{-1} and 20.6 ± 0.2 mg C l^{-1}, respectively. A high-temperature combustion system (Shimadzu TOC-5000) was used to obtain all DOC measurements. Using a Büchi Rotavapor at a vacuum setting of 27–30 mg Hg and a water bath temperature of 26–30°C, the NOM solutions were concentrated to 138 ± 3 and 175 ± 9 mg C l^{-1}, respectively (Table 1). The *p*NOM and *e*NOM were concentrated to a final volume of ~ 0.45 l. No contamination of the NOM was detected during the concentration procedure; final concentrations of NOM agreed to within 10% of the expected concentration given changes in volume and salt content (Table 1).

2.2. Sediment preparation

Approximately 1.5 kg of bulk sediment was saved during the extraction phase and stored frozen. In order to observe any size related adsorption differences the sediment was wet sieved into the following sizes: 250–63 μm (fine sand), 63–38 μm (coarse silt), < 38 μm (fine silt and clay; Table 2). Prior to fractionation the sediment was rinsed with distilled water to remove excess salt. Bulk and fractionated sediments were then freeze-dried and organics were removed by slow oxidation in an aerated oven at 350°C for 12 h (Keil et al., 1997). After cleaning, the quantity of remaining organic matter was estimated by CHN analysis to be less than 0.05% OC, and the solubility of this residual was within the sorption experimental error. The BET surface area of the samples was obtained using nitrogen gas with a Micromeritics ASAP-2010C surface area analyzer (Table 2). The dominant mineralogy of Puget Sound sediments is quartz, feldspars, and chlorites. Clay-sized fractions are dominated by quartz and expandable clays (e.g., montmorillonite; Brundage, 1960).

Two additional minerals were used in the adsorption and desorption experiments. Montmorillonite (standard number 48 W 1270) was obtained from Ward's Natural Science Establishment, and Iron(III) Oxide (Fe_2O_3; Puratronic grade 99.99%) was ob-

Table 2
Sinclair Inlet sediment data and data for the two mineral standards

	Fraction of total	TOC	TN	$(C:N)_{atomic}$	BET surface area (m^2 g^{-1})
250–63 μm	25	1.57	0.08	21.6	2.5
63–38 μm	50	1.19	0.07	19.2	2.7
< 38 μm	25	1.95	0.17	14.0	8.0
Bulk	NA	1.84	0.12	17.7	5.9
Montmorillonite	NA	NA	NA	NA	25.7
FeOxide	NA	NA	NA	NA	13.1

Grain size distribution (mass fraction in each size class), CHN results for each size class (TOC, TN, C:N ratio) and nitrogen-specific mineral SA data for each size class. NA is non-applicable.

tained from Alfa. The montmorillonite was homogenized with a ceramic mortar and muffled for 12 h at 350°C to remove organics. The average surface area was 26.6 m^2 g^{-1}. No further purification was done on the iron oxide, the average size was between 10 and 20 microns and the surface area was 13.1 m^2 g^{-1} (Table 2).

2.3. Adsorption and desorption isotherms

In order to assess the time necessary to reach steady state, an experiment was conducted in which multiple tubes were prepared at an initial *e*NOM concentration of 175 mg C l^{-1} (see below). Replicate tubes were incubated for varying amounts of time between 0 and 48 h. Results indicated that sorption reached stable values within 1 h and that incubating samples for longer periods of time did not significantly change adsorption densities (data not shown). For all subsequent adsorption studies, an incubation time of 2 h was used.

To determine whether changes in salinity (0–200‰) significantly altered the adsorption behavior of organic matter in sea water, two control experiments were conducted. The protein BSA, and *e*NOM that had been desalted by ultrafiltration (1000 Da membrane), were sorbed to montmorillonite at varying concentrations in a solution of constant salinity (25‰) and in a solution of increasing salinity (25–200‰; using sea salts). Sorption of BSA and desalted *e*NOM to montmorillonite was not affected by changes in salinity within the tested range (data not shown), indicating that the sorption isotherms generated were not likely to be significantly influenced by the changing salt concentrations.

Adsorption and desorption experiments were conducted using combinations of *p*NOM, *e*NOM, organic-free bulk sediment, sediment size fractions, montmorillonite and iron oxide. Prior to incubating NOM in the presence of mineral, a mineral slurry was prepared by adding 300 mg of sediment to 15 ml ultraviolet-oxidized sea water. Under constant vigorous stirring with a stir bar, 0.5 ml of slurry was pipetted into duplicate 4.5 ml solutions of either *p*NOM or *e*NOM (final concentration of solids; 2 g l^{-1}). The range of initial NOM concentrations was 0 to 175 mg l^{-1}. The tubes were vortex mixed and then shaken for 2 h. After incubation, the tubes were centrifuged for 20 min at $12\,500 \times g$, the supernatant was removed with a syringe, and then filtered through a pre-combusted Whatman GF/F filter into clean glass vials for subsequent DOC analysis. Isotherms were constructed by comparing the DOC concentrations at steady state to the sorbed NOM concentration calculated by difference between initial and final DOC concentration (e.g., Fig. 1).

Sediments from adsorption experiments with sorbed NOM were used for desorption experiments. Desorption measurements were conducted immediately following adsorption experiments. In no case did more than 24 h elapse between adsorption and desorption measurement, the average delay between adsorption and desorption was 12 h (overnight). Samples were stored cold at 2°C between experiments. For desorption, the ratio of solid to liquid was kept the same as in adsorption experiments. Ultraviolet-oxidized sea water (NOM concentrations < 0.05 mg C l^{-1}) was added to a wet bed of sediment from an adsorption experiment and the sediment was dispersed by vortex mixing. The tubes were then shaken for 2 h and centrifuged. The supernatant was removed, processed for DOC analyses as above, and replaced with clean water. This was repeated three times. The concentration of desorbed NOM was measured as the amount of DOC in the water at each step.

The cumulative sorptive properties of *p*NOM were evaluated by incrementally exposing *p*NOM to clean surfaces. Starting with an initial *p*NOM concentration of 123 mg C l^{-1}, sediment (38–63 μm) was added at a final concentration of 2 g l^{-1} and equilibrated for 2 h. After equilibration, the sediment was removed by centrifugation, a subsample was withdrawn for DOC analysis, and new sediment was added at the same solid:solution ratio. This procedure was repeated until DOC concentrations had levelled out and no more sorption was detectable. The NOM fraction remaining in the solution is functionally regarded as non-adsorbing. *e*NOM was not evaluated due to a lack of available material.

All adsorption and desorption experiments were conducted at 25°C in oxic conditions. No attempt was made to adjust the pH of the pore water or easily extracted solutions, and all adsorption/desorption experiments were conducted at a normal marine pH (~ 7.8).

2.4. Mathematical treatment of data

The adsorption data were fit to the Freundlich equation:

$$C_{ads} = K_f C_{dis}^n \quad (1)$$

where C_{ads} is the adsorbed concentration, C_{dis} is the dissolved concentration, K_f is the Freundlich adsorption coefficient which is related to the adsorption capacity of the mixture and n is the linearity coefficient. The linearity coefficient indicates whether sorption dynamics change as a function of solution concentration. If $n > 1$, sorption increases with increasing solution concentration. At $n < 1$, sorption decreases with increasing concentration (e.g., Langmuir-type isotherms). The Langmuir equation was not used because saturation of surfaces was not observed, and thus the Freundlich equation provides a better empirical fit to the data. Adsorption partition coefficients (K_d) for the linear portions of the isotherms (typically through the concentration range of 0–60 mg l^{-1}) were calculated using the standard least squares equation and are expressed in units of l g^{-1}.

Desorption data were treated in two ways. The total dataset for either *p*NOM or *e*NOM was regressed using the least squares equation where the slope is the desorption partition coefficient (K_{des}; l g^{-1}) and the *y*-intercept is a measure of the maximum amount of 'irreversible' sorption (assuming no curvature in the desorption isotherm). Additionally, individual desorption isotherms were modeled using the desorption isotherm equation presented by Gu et al., 1995:

$$C_{ads} = \frac{K_q C_{ads\,max} C_{dis}}{K_q C_{dis} + (C_{dis}/C_{dis\,max})^h} \quad (2)$$

where K_q is the surface excess-dependent affinity parameter, $C_{ads\,max}$ is the maximum amount of NOM adsorbed before commencement of desorption, $C_{dis\,max}$ is the maximum concentration of dissolved NOM before commencement of desorption, and h is the hysteresis coefficient. The parameter h is confined to a range of 0–1, where a value of zero represents completely reversible sorption, and one represents completely irreversible sorption given the conditions employed.

Since NOM is a heterogeneous mixture of different organic components, a multiple-component model was used to evaluate the coupled sorption/desorption data and the cumulative sorption data. For the coupled sorption/desorption data, it was assumed that sorption was reversible, and that any hysteresis between adsorption and desorption was due, in part, to loss of the least surface-reactive fractions when the equilibrated sediment was isolated from the water used for sorption and exposed to clean sea water at the beginning of the desorption experiment. Given these assumptions, two equations describing the sorption and desorption isotherms can be evaluated for the least number of terms that constrain both equations. For adsorption of a heterogeneous mixture of components,

$$K_{d(obs)} = \sum K_{d(i)} f_{i(t)} \quad (3)$$

where $K_{d(obs)}$ is the observed partition coefficient of the NOM, $K_{d(i)}$ is the partition coefficient of the i^{th} component, and $f_{i(t)}$ is the fraction of the total NOM in the system that is composed of component i. For desorption of a previously equilibrated mixture of heterogeneous components,

$$K_{des(obs)} = \sum K_{d(i)} f_{i(s)} \quad (4)$$

where $K_{des(obs)}$ is the observed desorption partition coefficient and $f_{i(s)}$ is the fraction of all sorbed NOM that is composed of component i in the system at the beginning of the desorption experiment. The two equations can be solved for the fewest components that describe both equations.

For the cumulative sorption experiment, the shape of the resultant sorption profile can be modeled as,

$$C_{dis} = \sum f_i^{(-K_{d(i)}X)} \quad (5)$$

where X is the cumulative mass of sediment exposed to the NOM. Mathematically, this is the equivalent of multi-G modeling of organic matter diagenesis. Discrimination of significant trends from the data set was made by comparing standard deviations of various parameters using Student's *t*-test.

3. Results

To generate isotherms, a 2 h incubation period was used to allow the NOM to come into steady

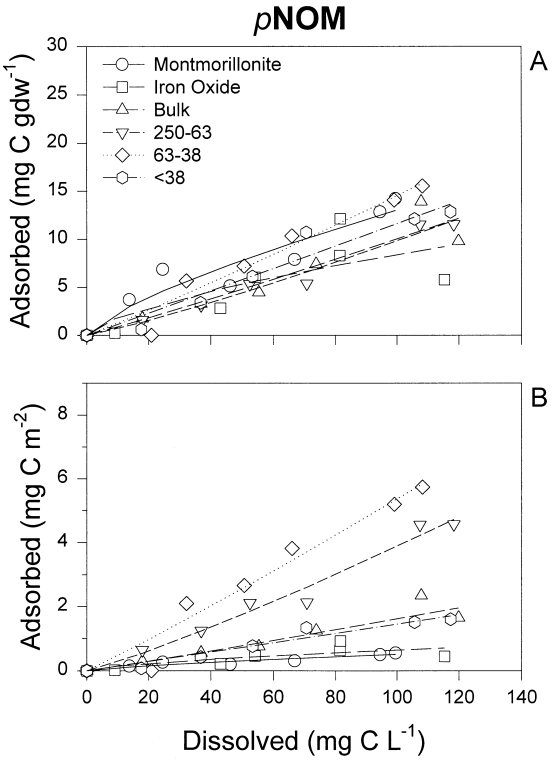

Fig. 1. Pore water NOM adsorption isotherms for the various mineral classes. Lines represent Freundlich isotherm model fits to the adsorption data. Data points represent the average of duplicate or triplicate analyses at each solution concentration. (A) Plotted normalized to sediment weight. (B) Plotted normalized to sediment surface area.

state. Previous studies have shown that most model compounds and riverine NOM come to steady state within minutes when reacted with surfaces (Kirchman et al., 1989; Wang and Lee, 1993; Day et al., 1994). We tested the validity of this assumption by monitoring sorption densities over a 48 h period and observed that sorption did indeed reach constant levels in minutes. Thus, while the potentially heterogeneous composition of NOM may be undergoing competitive exchange (Gu et al., 1996), steady-state values for total NOM sorbed can be reliably obtained by using a 2 h reaction time. During sample preconcentration, salts were also concentrated, potentially complicating NOM sorption isotherms because each NOM concentration had a corresponding salinity and ionic strength. The possible influence of solution ionic strength was evaluated by sorbing desalted *e*NOM and a protein to montmorillonite under both constant and changing salinities. Although the isotherms for the protein and the desalted *e*NOM were very different from each other, neither the protein nor the *e*NOM exhibited a change in isotherm as a result of changing salinity, indicating that there was no discernible salt effect (data not shown).

Adsorption isotherms for *p*NOM and the Sinclair Inlet mineral size classes, montmorillonite and iron oxide are nearly linear over a DOC concentration range of 0–120 mg C l^{-1}(Fig. 1a). On a mass-weighted basis the substrates adsorb approximately the same amount of *p*NOM. Freundlich coefficients (K_f) range from 0.05–0.43 and linearity coefficients (n) cluster in a range from 0.65–1.15 (Table 3). Partition coefficients (K_d) for the *p*NOM are uniform and range from 8×10^{-3} ml mg^{-1} to 12×10^{-3} ml mg^{-1}(Table 3). On a mineral surface area-basis (expressed in units of mg C m^{-2}), the amount sorbed is highest for the 38–63 and 63–250 μm fractions (Fig. 1b). The bulk sediment and the <38 μm fraction sorb intermediate amounts and the montmorillonite and iron oxide sorb the least.

Sorption isotherms for *e*NOM are not as uniform as the *p*NOM isotherms (Fig. 2). Only sorption of *e*NOM to the iron oxide, <38 and 38–63 μm fractions resulted in isotherms that were similar to

Table 3
Results of adsorption isotherms for the *p*NOM and the *e*NOM

		K_f	n	K_d
*p*NOM	clean bulk sediment	0.08	1.06	0.12
	63–250 μm	0.05	1.15	0.10
	38–63 μm	0.11	1.07	0.15
	<38 μm	0.11	1.00	0.12
	Montmorillonite	0.43	0.74	0.12
	Iron oxide	0.41	0.65	0.13
*e*NOM	clean bulk sediment	1.82	0.38	0.08
	63–250 μm	0.98	0.42	0.09
	38–63 μm	0.08	1.13	0.01
	<38 μm	0.04	1.19	0.10
	Montmorillonite	0.07	1.36	0.33
	Iron Oxide	0.91	0.59	0.22

Freundlich adsorption coefficients (K_f) and partition coefficients derived from least squares linear regression (K_d) are expressed in units of l g^{-1}. One standard deviation was typically less than ten percent of the value. The linearity coefficient of the Freundlich isotherm is expressed as n, and has a standard deviation of approximately fifteen percent of the estimated value.

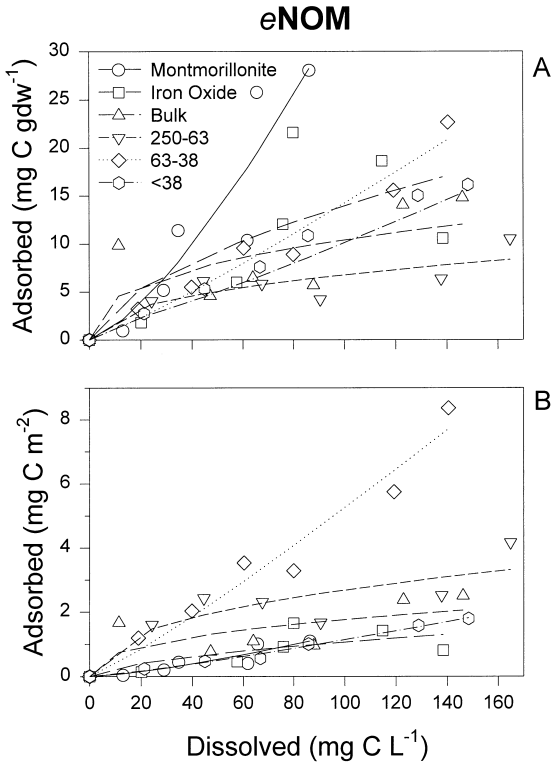

Fig. 2. Easily extracted NOM adsorption isotherms for the various mineral classes. Lines and data as in Fig. 1. (A) Plotted normalized to sediment weight. (B) Plotted normalized to sediment surface area.

those for *p*NOM. Sorbed *e*NOM concentrations reach a plateau on the 63–250 μm size class (Fig. 2a), which results in low linearity coefficients (Table 3). On a carbon weight basis, *e*NOM was most reactive toward the montmorillonite (Fig. 2a). When normalized to mineral surface area, similarly to the *p*NOM, sorption of *e*NOM was highest on the 38–63 and 63–250 μm fractions and lowest on the montmorillonite and iron oxide (Fig. 2b).

Desorption experiments were conducted using sediment containing sorbed NOM at the end of the adsorption experiments. Typically three concentrations were chosen for consecutive desorption (Table 4). In all cases a hysteresis was observed between the adsorption and desorption steady state values (Fig. 3a). Despite sorption to different minerals and size fractions, all the desorption data curve toward the intercept in a manner suggestive of reversible sorption. To determine if sorption was reversible under the conditions employed, the desorption data were treated in two ways. Data were fit to the desorption isotherm described by Gu et al., 1995. This model was chosen because the desorption data appear to curve toward the origin in a manner consistent with a Langmuir-style isotherm (Fig. 3). Fits to this model provide a hysteresis coefficient, *h* (Gu et

Table 4
Desorption affinity coefficients (K_{des}; mg l^{-1}), derived from least squares linear regression, for experiments in which sequential desorption steps were conducted

	Substrate	$_i$DOC	K_{des}
*p*NOM	clean bulk sediment	165	0.18 ± 0.11
		150	0.14 ± 0.05
		75	0.28 ± 0.03
	63–250 μm	165	0.20 ± 0.06
		150	0.17 ± 0.08
		75	0.28 ± 0.08
	38–63 μm	165	0.19 ± 0.05
		150	0.27 ± 0.01
		75	0.30 ± 0.04
	> 38 μm	165	0.35 ± 0.03
		150	0.24 ± 0.07
		75	0.35 ± 0.07
	Montmorillonite	165	0.10 ± 0.01
		150	0.24 ± 0.05
	Iron Oxide	165	0.28 ± 0.11
		150	0.32 ± 0.11
		75	0.65 ± 0.07
	Combined average	N/A	0.45 ± 0.01
*e*NOM	clean bulk sediment	175	0.15 ± 0.05
		150	0.10 ± 0.03
	63–250 μm	175	0.14 ± 0.03
		150	0.39 ± 0.05
		100	0.11 ± 0.05
	38–63 μm	175	0.20 ± 0.03
		150	0.20 ± 0.06
		75	0.30 ± 0.03
	< 38 μm	175	0.21 ± 0.03
		150	0.21 ± 0.02
		75	0.30 ± 0.08
	Montmorillonite	175	0.17 ± 0.04
		150	0.15 ± 0.04
	Iron Oxide	175	0.37 ± 0.01
		150	0.34 ± 0.27
		75	0.62 ± 0.23
	Combined average	N/A	0.48 ± 0.02

$_i$DOC is the initial concentration of DOC added to the mineral phase prior to desorption (the initial sorbed NOM concentration was calculated from this value by difference after sorption—see Section 2). Combined averages derived from least squares linear regression of combined desorption plots in Fig. 3.

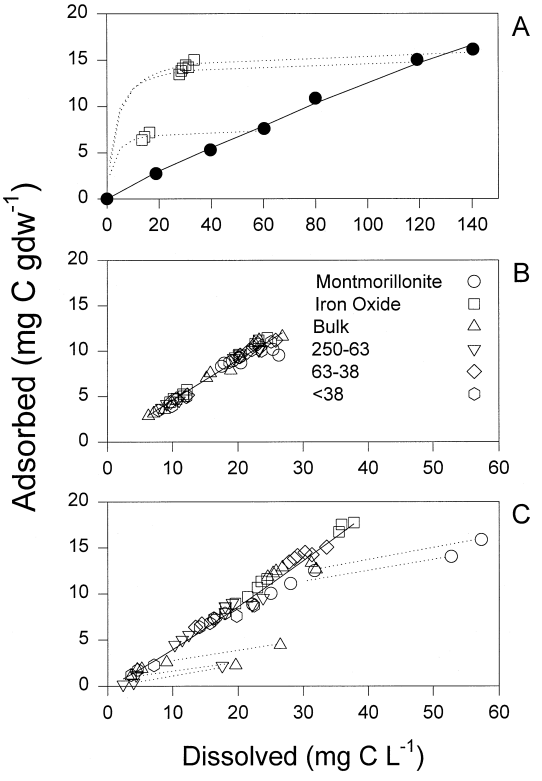

Fig. 3. Desorption isotherms for *p*NOM and *e*NOM. (A) Isotherms for *e*NOM adsorbed to and desorbed from < 38 μm sediment. The dashed lines are curve fits generated by using Eq. (2). The solid line denotes the Freundlich fit to the adsorption isotherm. (B) Freundlich fit to all the desorption data conducted using *p*NOM and various mineral classes. (C) Same as B except data plotted are for desorption isotherms of *e*NOM. Dashed lines mark data sets that contain points that do not all fall along the visual trend.

al., 1995). Hysteresis coefficients range from 0–0.1. This suggests that the desorption was largely reversible, but allows for some irreversible sorption, especially by the *e*NOM.

Since all the *p*NOM and *e*NOM desorption data appear to fall along a single line regardless of solid substrate, single Freundlich isotherms were calculated using all the desorption data for the *p*NOM or *e*NOM (Fig. 3b and c). Application of the Freundlich equation to the desorption isotherms provides $K_{f(des)}$ and n_{des} values of 0.3 and 1.05 for *p*NOM and 0.4 and 1.0 for *e*NOM, respectively. Desorption partition coefficients (K_{des}) for both *p*NOM and *e*NOM are 0.7 ± 0.1 and *y*-axis intercepts are not significantly different from zero (Fig. 3b,c). These two observations also suggest that desorption was largely reversible.

Considering that NOM is a heterogeneous mixture of components, and assuming that sorption is largely reversible (as suggested by both the above treatments of the desorption data) the combined adsorption/desorption data can be coupled and treated together. During sorption, the fraction of NOM remaining in solution at steady state is a product of the K_d's and mass fractions of each component in the mixture and the porosity of the solution. In a simple system, it is likely to be dominated by the components with the lowest K_d's (unless the high K_d components are present in large excess). When the NOM in solution is removed and the desorption experiment is started by adding NOM-free solution, only NOM that was sorbed can be released into the new solution. In a simple system, this sorbed component will be rich in components with higher K_d's (unless the low K_d components are in large excess). The result is that the desorption isotherm shifts from the sorption isotherm to represent a balance of the components with higher K_d's (an apparent hysteresis is observed). That is, the sorption isotherm is an average of all the NOM, whereas the desorption isotherm is an average of only the components on the surface at steady state, which will likely be dominated by components with higher K_d's than the average of the bulk NOM. Using Eqs. (3) and (4), the *p*NOM and *e*NOM data were independently evaluated for the least number of component fractions that would satisfactorily ($\pm 5\%$) model the data. For the *p*NOM, two components with average K_d's of 3.3 and 0.02 and mass fractions of 0.19 and 0.81 best fit the data. For the *e*NOM, similar values of $K_d = 3.15$ and 0.02 and mass fractions of 0.20 and 0.80 were estimated.

When *p*NOM was equilibrated incrementally with sediment, dissolved NOM concentrations decreased rapidly for the first 6 g l^{-1} of added sediment, but then diminished (Fig. 4). Approximately 75% of the *p*NOM did not sorb to the surfaces. Fitting the data to Eq. (5) results in a mixture of NOM components that can be constrained by 2 components with K_d's of 3.25 and 0.02 and mass fractions of 0.21 and 0.79. These estimates are the same as that predicted based on the coupled sorption/desorption data and suggest

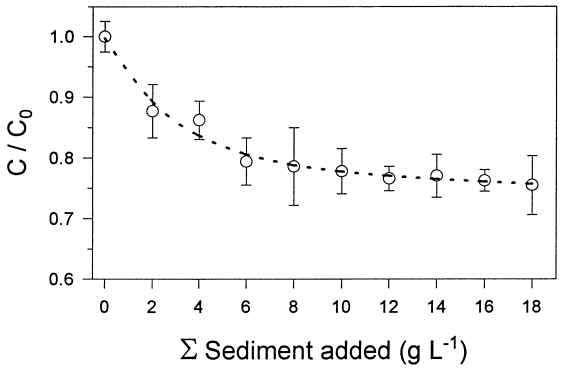

Fig. 4. Incremental sorption of *p*NOM to sediment in the 38–63 μm size fraction. Initial concentration of *p*NOM was 123 mg C l^{-1} and pH was held constant at $\sim$7.8. C/C_0 is the fraction of *p*NOM in solution at any step. The curve fit represents the summed sorption of a two-component mixture containing components with K_d's of 3.25 and 0.02 and mass fractions of 0.21 and 0.79.

that the heterogeneity of *p*NOM can be described by two components with very different K_d's.

4. Discussion

The sorptive behavior of sedimentary NOM contributes to its microbial reactivity, physical partitioning and mobility, and ultimately to its preservation (Wang and Lee, 1993; Henrichs and Sugai, 1993). While previous studies have investigated the effects of organic-mineral interactions using model compounds (Gordon and Millero, 1985; Sugai and Henrichs, 1992), there have been no prior evaluations of the sorptive characteristics of sedimentary dissolved NOM. This study evaluates the surface reactivity of pore water NOM after isolation and concentration of the NOM.

Except for slight saturation of sorption to iron oxide, sorption of *p*NOM did not change substantially with changes in sediment mineralogy or grain size, and was independent of mineral surface area (Fig. 1; Table 3). This suggests that the *p*NOM was not substrate-specific in its sorptive behavior and was not sorbing in direct response to available surface. The dominant mineralogies of the sediment size fractions (quartz, feldspars and montmorillonite) would all have a net negative charge before the addition of the NOM (Stumm, 1992). Only the iron oxide (Fe_2O_3) would have a charge that was either nearly neutral in sea water at a pH of $\sim$7.8 (Stumm, 1992). Coincidentally, the only substrate with a significant deviation was the iron oxide. It may be that sorption of the *p*NOM to iron oxide was slightly lower than for the other minerals due to the difference in net surface charge. Skoog et al. (1996) hypothesized that since the sorption of organic matter to oxides was strongly pH dependent and decreases with increasing pH, sorption of NOM to oxides at a pH $\sim$7.8 would be low. However, Keil et al. (1998) compared the molecular composition of sedimentary organic matter in sediment size fractions to the dominant mineralogies of each fraction and determined that there was no clear mineralogical effect. Although surfaces were cleaned prior to experimentation, it is possible that residual oxide coatings on the surfaces contributed to their similar sorptive characteristics. Another explanation for the similarity in sorption across the mineral size classes is that a strongly-sorbed minor component of the NOM dominates initial sorption and determines the remaining sorptive properties. Finally, the results presented here are also consistent with nucleation-driven precipitation, in which the presence of added sediment helps drive precipitation of the NOM. The relatively large scatter in the data, especially for the *p*NOM, do not allow discrimination between sorption and precipitation, but the conclusions drawn for the concentrated NOM solutions remain valid regardless of which mechanism is operating.

Partition coefficients for *p*NOM sorption are low and average only 0.1 l g^{-1} (Table 3). Most compounds that have been evaluated for their sorptive characteristics have much higher partition coefficients in sea water (Henrichs and Sugai, 1992). A common range for partition coefficients (ignoring any solid-to-solution ratio variations) is 0.1–1000 (Henrichs and Sugai, 1992). Thus, relative to many model compounds, the average K_d for *p*NOM suggests a component that is not strongly surface reactive.

Overall, the sorptive characteristics of the *e*NOM were similar to those of *p*NOM in that partition coefficients were low, Freundlich linearity coefficients were near one, and the iron oxide sorbed

slightly lower quantities than the other mineral phases. However, both the bulk sediment and the 250–63 μm size fraction had isotherms that leveled out with respect to sorption of NOM (Fig. 2). This indicates that the surfaces of these two sediment fractions were becoming saturated with NOM. Interestingly, the maximum quantity of *e*NOM sorbed by these two fractions (5–10 mg C g^{-1}) is roughly equivalent to the common organic carbon content of many sandy sediments.

The *p*NOM and *e*NOM were isolated from an anoxic sediment, but sorption experiments were conducted under oxic conditions. There is no physiochemical reason why redox conditions should affect the sorptive properties of organic matter (Stumm, 1992). However, Wang and Lee, 1993 suggested that there may be a redox effect during the partitioning of organic matter in marine sediments. They observed higher amounts of lysine sorption to natural sediments under oxic conditions, suggesting that reducing sediments may, for some reason, sorb less organic matter than oxic sediments. Rather than being due to a direct redox effect, changes in sorption are most likely related to changes in mineral characteristics that are redox-sensitive. Under reducing conditions, the primary forms of amorphous mineral phases are sulfides, which exhibit low surface reactivities (Stumm, 1992; Luther, personal communication), and are likely to contribute substantially to sediment surface area. Under oxic conditions, amorphous mineral phases are dominated by oxy-hydroxides, which tend to have high surface reactivities depending on pH (Mazet et al., 1990; Schlautman and Morgan, 1994). The affinity of *p*NOM and *e*NOM to sulfides was not assessed here. However, there was little difference in the sorption characteristics of the NOM pools as a function of mineralogy. This suggests that sorption to sulfides might also have been similar, although that remains to be evaluated.

In order to evaluate sorption reversibility, consecutive desorption experiments were conducted. For all the experiments, a hysteresis was observed between the adsorption and desorption isotherms (Fig. 3a). At first glance, it appears that the sorbed NOM was not readily desorbed and that there was an irreversibly bound fraction of NOM. However, there is curvature in the isotherms, and application of a desorption model fit to the data (Gu et al., 1995) illustrates that the desorption isotherms have a strong inflection toward the origin, suggesting that although the sorption and desorption paths are distinct, most NOM is reversible sorbed (Fig. 3a; Table 4). This observation also comes from the single characteristic line that both *p*NOM and *e*NOM data fall along (Fig. 3b, c). Extrapolation of the line to the *y*-intercept yields an intercept indistinguishable from zero, indicating that the NOM was reversibly sorbed. The tight fit of both the *p*NOM and *e*NOM desorption data to a single line suggests that the desorbing NOM is similar for the two original NOM fractions. This is evidence that *p*NOM and *e*NOM are undergoing exchange and comprise fractions of the same NOM pool.

Hystereses are typically interpreted as the result of changes in sorptive mechanism between the time of sorption and desorption that result in decreased kinetics of desorption relative to adsorption. However, for heterogeneous NOM, hysteresis may result from the heterogeneity in the system and the methodology employed. Fits of the data to a multicomponent model suggest that the hysteresis result from a mixture typified by two components with very different K_d's. We do not suggest that there are only two components in the NOM isolates, rather, the calculation is intended to illustrate that apparent hysteresis can be explained by NOM heterogeneity. Extension of these data to a continuous distribution model (Perdue, 1990) would likely illustrate a continuum of K_d's with decreasing abundance as K_d increases. The functionality of a two-component 'solution' to the dataset is that the rough proportions of surface-reactive and surface-indifferent components can be gauged. Similar results are obtained in the cumulative sorption experiment (Fig. 4). Both analyses suggest that approximately 75% of the *p*NOM has a $K_d < 0.02$ and that $\sim$25% has a K_d in the range of one or more.

In summary, *p*NOM and *e*NOM have similarly low partition coefficients for sorption and identical desorption isotherms and desorption partition coefficients. This supports the hypothesis that pore waters contain NOM components that are poorly reactive toward surfaces, but because of the high solid-to-solution ratios observed in sediments, a large component is reversibly sorbed, and this component buffers and influences the concentrations and mobilities of NOM in marine pore waters. The results of this

study are consistent with earlier work (Henrichs, 1993) on organic matter in marine sediments and strengthen the accumulating evidence that sorption is an important component that influences the potential fate of NOM in marine sediments. Our results illustrate how closely the solid and solution NOM pools can interact, and suggest that the diffusion of *p*NOM through pore waters may be hindered by organic–organic interactions which are not routinely accounted for in studies of NOM diffusion. While experiments using either tracer compounds or bulk NOM are a useful and necessary step toward understanding the dynamics of NOM in marine sediments, further work must focus on identifying specific components of NOM in complex mixtures and evaluating their surface reactivities (and the effect of surface interaction) under in situ conditions. Additionally, current knowledge of the surface reactivity of the strongly surface-associated NOM is inadequate. Further elucidation of the exact mechanisms of NOM-sediment interactions will require examination of these aspects.

Acknowledgements

We thank Annelie Skoog, Anthony Aufdencampe, John Hedges and the UW-AOG group (http://boto.ocean.washington.edu/aog/index.html) for fruitful discussion of this work, and Elizabeth Tsamakis for help collecting the samples. We also thank Patsy Cline for sound advice. This research was supported by NSF grants to RGK and is contribution number 2192 from the University of Washington School of Oceanography.

References

Brundage, W.L., 1960. Recent sediment of the Nisqually river delta, Puget Sound, Washington. M.S. Thesis, University of Washington.

Day, G.M., Hart, B.T., McKelvie, I.D., Beckett, R., 1994. Adsorption of natural organic matter onto goethite. Colloids and Surfaces, pp. 1–13.

Gordon, A.S., Millero, F.J., 1985. Adsorption mediated decrease in the biodegradation rate of organic compounds. Microbiol. Ecol. 11, 289–298.

Gu, B., Schmitt, J., Chen, Z., Liang, L., McCarthy, J.F., 1995. Adsorption and desorption of different organic matter fractions on iron oxide. Geochim. Cosmochim. Acta, pp. 219-229.

Gu, B., Mehlhorn, T.L., Liang, L., McCarthy, J.F., 1996. Competitive adsorption, displacement, and transport of organic matter on iron oxide: Part 1. Competitive adsorption. Geochem. Cosmochim. Acta 60 (11), 1943–1950.

Hedges, J.I., 1977. The association of organic molecules with clay minerals in aqueous solutions. Geochim. Cosmochim. Acta 41, 1119–1123.

Hedges, J.I., Keil, R.G., 1995. Sedimentary organic matter preservation: an assessment and speculative synthesis. Marine Chem. 49, 81–115.

Henrichs, S.M., 1993. Early diagenesis of organic matter: the dynamics (rates) of cycling of organic compounds. Plenum, New York, pp. 101–117.

Henrichs, S.M., 1995. Sedimentary organic matter preservation: an assessment and speculative synthesis—a comment. Marine Chem. 49, 127–136.

Henrichs, S.M., Sugai, S.F., 1993. Adsorption of amino acids and glucose by sediments of Resurrection Bay, Alaska, USA: functional group effects. Geochim. Cosmochim. Acta 57, 823–835.

Henrichs and Sugai, 1992.

Keil, R.G., Tsamakis, E.C., Fuh, C.B., Giddings, J.C., Hedges, J.I., 1994. Mineralogical and textural controls on the organic composition of coastal marine sediments: hydrodynamic separation using SPLITT-fractionation. Geochim. Cosmochim. Acta 58 (2), 879–893.

Keil, R.G., Tsamakis, E., Wolf, N., Hedges, J.I., Goni, M., 1997. Relationships between organic carbon preservation and mineral surface area along the Amazon fan (Sites 932A and 942A). In: Flood, R.D., Piper, D.J.W., Klaus, A., Peterson, L.C. (Eds.), Proc. of the Ocean Drilling Program, Scientific Results, Vol. 155, pp. 531–538.

Keil, R.G., Tsamakis, E., Giddings, J.C., Hedges, J.I., 1998. Biochemical distributions (amino acids, neutral sugars and cupric oxide oxidation products) among size–classes of modern marine sediments. Geochim. Cosmochim. Acta, in press.

Kirchman, D.L., Henry, D.L., Dexter, S.C., 1989. Adsorption of proteins to surfaces in sea water. Marine Chem. 27, 201–217.

Mayer, L.M., 1994. Surface area control of organic carbon accumulation in continental shelf sediments. Geochim. Cosmochim. Acta 58 (4), 1271–1284.

Mazet, M., Angbo, L., Serpaud, B., 1990. Adsorption of humic acids onto preformed aluminum hydrooxide flocs. Water Res. 24 (12), 1509–1518.

Pedersen, T.F., 1995. Sedimentary organic matter preservation: an assessment and speculative synthesis—a comment. Marine Chem. 49, 117–119.

Perdue, E.M., 1990. Modeling the acid–base chemistry of organic acids in laboratory experiments and fresh waters. In: Perdue, E.M., Gjessing, E.T. (eds.), Organic Acids in Aquatic Ecosystems. Wiley, pp. 111–126.

Sansone, F.J., Andrews, C.C., Okamoto, M.Y., 1987. Adsorption of short-chain organic acids onto nearshore marine sediments. Geochim. Cosmochim. Acta 51, 1889–1896.

Schlautman, M.A., Morgan, J.J., 1994. Adsorption of aquatic

humic substances on colloidal-size aluminum oxide particles: influence of solution chemistry. Geochim. Cosmochim. Acta 58 (20), 4293–4303.

Skoog, A., Hall, P.O.J., Hulth, S., Paxeus, N., van der Loeff, M.R., Westerlund, S., 1996. Early diagenetic production and sediment–water exchange of fluorescent dissolved organic matter in the coastal environment. Geochim. Cosmochim. Acta 60 (19), 3619–3629.

Stumm, W., 1992. Chemistry of the Solid–Water interface. Wiley-Interscience, 428 pp.

Sugai, S.F., Henrichs, S.M., 1992. Rates of amino acid uptake and mineralization on Resurrection Bay (Alaska) sediments. Marine Ecol. Prog. Ser. 88, 129–141.

Wang, X.-C., Lee, C., 1993. Adsorption and desorption of aliphatic amines, amino acids and acetate by clay minerals and marine sediments. Marine Chem. 44, 1–23.